The Journal of Immunology

Low Thymic Activity and Dendritic Cell Numbers Are Associated with the Immune Response to Primary Viral Infection in Elderly Humans

Axel Ronald Schulz, Julia Nora Mälzer, Cristina Domingo, Karsten Jürchott, Andreas Grützkau, Nina Babel, Mikalai Nienen, Tomas Jelinek, Matthias Niedrig and Andreas Thiel

J Immunol 2015; 195:4699-4711; Prepublished online 12 October 2015;
doi: 10.4049/jimmunol.1500598
http://www.jimmunol.org/content/195/10/4699

The Journal of Immunology is published twice each month by
The American Association of Immunologists, Inc.,
1451 Rockville Pike, Suite 650, Rockville, MD 20852

Print ISSN: 0022-1767 Online ISSN: 1550-6606.

Low Thymic Activity and Dendritic Cell Numbers Are Associated with the Immune Response to Primary Viral Infection in Elderly Humans

Axel Ronald Schulz,*,†,[1] Julia Nora Mälzer,*,[1] Cristina Domingo,‡ Karsten Jürchott,§ Andreas Grützkau,† Nina Babel,¶ Mikalai Nienen,¶ Tomas Jelinek,‖ Matthias Niedrig,‡ and Andreas Thiel*

Immunological competence declines progressively with age, resulting in increased susceptibility of the elderly to infection and impaired responses to vaccines. Underlying mechanisms remain largely obscure as they have been related to complex, individual systemic immune properties that are challenging to investigate. In this study, we explored age-related changes in human immunity during a primary virus infection experimentally induced by immunization with live-attenuated yellow fever (YF) vaccine. Applying detailed serology, advanced FACS analysis, and systems biology, we discovered that aged subjects developed fewer neutralizing Abs, mounted diminished YF-specific $CD8^+$ T cell responses, and showed quantitatively and qualitatively altered YF-specific $CD4^+$ T cell immunity. Among numerous immune signatures, low in vivo numbers of naive $CD4^+$ recent thymic emigrants and peripheral dendritic cells correlated well with reduced acute responsiveness and altered long-term persistence of human cellular immunity to YF vaccination. Hence, we reveal in this article that essential elements of immune responses such as recent thymic emigrants and dendritic cells strongly relate to productive immunity in the elderly, providing a conceivable explanation for diminished responsiveness to vaccination with neoantigens and infection with de novo pathogens in the aged population. ***The Journal of Immunology*****, 2015, 195: 4699–4711.**

With increasing age, the human immune system undergoes a complex transformation leading to a decline in immunological competence associated with severe infections, malignancies, and autoimmunity at advanced age (1–3). Underlying mechanisms of immunological aging are mostly studied in animal models (4, 5), but the direct translation of these results to humans is complicated by the much higher life expectancy and individual systemic immune properties (6, 7). Further knowledge about the aged immune system has been obtained by comparing young and aged immune systems in the steady-state (8) or after secondary, booster vaccinations, such as tetanus or influenza (9, 10). However, the human immune response to an entire primary acute infection, from inoculation to complete resolution, has not been analyzed in elderly people in detail until now.

It has been theorized that age-related loss of naive T cells and thymic involution (11–13), as well as an aged innate immune system (14), could compromise immune responses in de novo challenges. But whether such age-related qualitative and quantitative cellular alterations affect a primary immune response has not yet been demonstrated directly in humans. We approached this issue using yellow fever (YF) vaccination fever as a model for a primary infection in humans (15, 16). The vaccine contains the live-attenuated YF virus 17D (YFV-17D) strain, which is able to infect human cells productively (17), causing a full acute immune response (18). The monovalent vaccine has been proved to be extremely effective with a seroconversion rate of 99% and may confer lifelong immunity (19). Despite its excellent safety record, rarely, unrestricted replication of the vaccine virus can lead to potentially fatal serious adverse events (20). Increased risk for YF-induced serious adverse events (YF-SAE) in vaccinees with thymus diseases (21) or at advanced age (>60 y) (22) indicates an involvement of immunological impairments in these groups.

In this study, we assessed and compared the complete immune response after primary YF vaccination in young and elderly volunteers. Detailed FACS analysis allowed us to detect age-related differences at multiple layers of the vaccine-induced immune response, which we correlated with immune signatures before and after vaccination. By this we sought to understand the impact of immunosenescence in the context of a primary infection in humans

*Regenerative Immunology and Aging, Berlin-Brandenburg Center for Regenerative Therapies, Charité University Medicine, Campus Virchow-Klinikum, 13353 Berlin, Germany; †Immune Monitoring Core, German Rheumatism Research Centre Berlin (a Leibniz Institute), D-10117 Berlin, Germany; ‡Center for Biological Threats and Special Pathogens 1 – Highly Pathogenic Viruses, Robert Koch Institute, 13353 Berlin, Germany; §Systems Biology of Infectious Diseases, Berlin-Brandenburg Center for Regenerative Therapies, Charité University Medicine, Campus Virchow-Klinikum, 13353 Berlin, Germany; ¶Renal and Transplant Research Unit, Berlin-Brandenburg Center for Regenerative Therapies, Charité University Medicine, Campus Virchow-Klinikum, 13353 Berlin, Germany; and ‖Berlin Center for Travel and Tropical Medicine, 10117 Berlin, Germany

[1]A.R.S. and J.N.M. contributed equally to this work.

ORCIDs: 0000-0002-5106-0148 (A.R.S.); 0000-0002-5678-1956 (M. Nienen); 0000-0001-7965-4872 (M. Niedrig).

Received for publication March 12, 2015. Accepted for publication September 21, 2015.

This work was supported by German Federal Ministry of Education and Research network PRIMAGE Grant 0315895A/B, German Federal Ministry of Education and Research project EPILYZE Grant 031A191E, and the Berlin-Brandenburg Center for Regenerative Therapies.

Address correspondence and reprint requests to Axel Schulz, Immune Monitoring Core, German Rheumatism Research Centre Berlin, Chariteplatz 1, D-10117 Berlin, Germany. E-mail address: axel.schulz@drfz.de

The online version of this article contains supplemental material.

Abbreviations used in this article: DC, dendritic cell; mDC1, type I $CD11c^+$ myeloid DC; MWW, Mann–Whitney *U*; PCA, principal component analysis; pDC, plasmacytoid DC; PRNT90, plaque reduction neutralization test 90; RTE, recent thymic emigrant; RT-PCR, real-time PCR; WNV, West Nile flavivirus; YF, yellow fever; YF-SAE, YF-induced serious adverse event; YFV-17D, YF virus 17D.

and to identify key signatures crucially affecting vaccination outcome in the elderly.

Materials and Methods

Vaccination and study cohort

Approval for this study was obtained from the ethics committee of the Faculty of Medicine–Charité, Humboldt University, Berlin, Germany. After informed consent and prior vaccination, sera of 26 volunteers were analyzed for potentially cross-reactive Abs against flaviviruses by the anti-flavivirus mosaic indirect immunofluorescence assay (EUROIMMUN, Lübeck, Germany), performed according to the manufacturer's protocol. Two donors showed tick-borne encephalitis virus-specific Abs and hence were omitted from analysis. Another donor retrospectively demonstrated unusual immunological features (high steady-state T cell activation) preventing proper evaluation and was therefore excluded from analysis as well. The remaining 23 volunteers were assigned into two age groups: young (11 donors, 20–30 y, median age 26 y, 5 female/6 male) and elderly (12 donors, 55–70 y, median age 60 y, 5 female/7 male). The upper age limit for participation was 70 y set by the ethical approval. Health status and current medication was assessed by questionnaire to exclude individuals with acute illness, history of cancer, autoimmune disease, allergies, or innate or acquired immunosuppression. Two of the elderly subjects were on medication for hypertension, one patient for diabetes mellitus type 2 and the other patient for benign prostatic hyperplasia. Furthermore, we ensured that volunteers were neither anemic nor lymphopenic before or during the study. Immunization was performed by a single s.c. injection of YFV-17D vaccine (Stamaril; Sanofi Pasteur MSD, Berkshire, U.K.). Any adverse reactions (erythema, swelling, myalgia, fever) were documented. Fifty milliliters of venous blood was drawn immediately before vaccination (day 0) and at eight further time points [days 2 (only donors 15–27), 4, 7, 10, 14, 17, 21, and 28] after vaccination into sodium heparin, serum gel, or EDTA tubes (BD Biosciences, Plymouth, U.K.). The study was run in three individual rounds [round I (donors 1–6), round II (donors 8–14), and round III (donors 15–27, additional study day 2)] and the obtained data sets were cross-checked for variability between runs before being merged for analysis. To study long-term YF-specific memory formation and stability, we collected in each case 50 ml venous blood from 19 of 23 vaccinees reinvited 33 (donors 1–6), 30 (donors 8–14), or 20 (donors 15–27) months after vaccination. Heparinized blood was processed and analyzed directly. Sera were stored at −80°C until use.

Detection of serum viremia with quantitative real-time PCR

Sera were tested for the presence of YFV-17D genomes at days 0, 2, 4, 7, and 10 after vaccination by quantitative real-time PCR (RT-PCR) as described elsewhere (23). A serial dilution of in vitro–generated viral RNA of known concentration was simultaneously run to standardize the measurement. The assay has a limit of detection of 0.8 PFU/ml (95% CI).

Plaque reduction neutralization test

Plaque reduction neutralization test 90 (PRNT90) assays of stored sera from all study time points were carried out according to the protocol established by Reinhardt (24). The 90% neutralization titers were calculated according to Reed and Muench (25).

CMV and EBV serology

Specific IgG responses against CMV and EBV were measured in day 0 sera of all vaccinees. Sera were automatically analyzed with the CMV or EBV IgG-Elisa PCS (Medac, Wedel, Germany) on an ELISA processor BEP III (Siemens, Erlangen, Germany).

Serum cytokine analysis

Serum IFN-γ was analyzed by a special-order human 8-plex assay (Meso Scale Discovery, Rockville, MD). Thawed sera were cleared by centrifugation at 4000 × *g*, 4 min, 4°C, diluted 2-fold, and analyzed in duplicates according to the manufacturer's protocol on a MESO QuickPlex SQ 120.

Complete blood count

Complete blood counts were performed on freshly collected EDTA blood, analyzed by the automated cell counter Sysmex XE-5000 (Sysmex, Kobe, Japan). Absolute whole blood counts of leukocytes, lymphocytes, monocytes, basophils, eosinophils, and neutrophils were determined.

Isolation of PBMCs

PBMCs were isolated from freshly drawn heparinized whole blood in 50 ml Leucosep tubes (Greiner, Kremsmünster, Austria) filled with 14 ml Ficoll-Hypaque (LSM 1077; PAA Laboratories, Pasching, Austria) according to the manufacturer's protocol.

Flow-cytometric analysis

Analysis of absolute frequencies of leukocyte populations in peripheral blood. To determine absolute counts of the analyzed leukocyte populations in freshly drawn peripheral blood, we incubated 50 μl heparinized whole blood for 15 min at room temperature with 50 μl fluorescence-labeled mAb mixture [anti-CD3 (OKT3), anti-CD4 (OKT4; both Biolegend, San Diego, CA), anti-CD8 (RPA-T8; eBioscience, San Diego, CA), anti-CD14 (M5E2), anti-CD45 (2D1), anti-CD56 (NCAM16.2; all BD Biosciences, San Jose, CA), anti-CD19 (Bu-12; Deutsches Rheumaforschungszentrum, Berlin, Germany), and anti-BDCA2 (AC144; Miltenyi, Bergisch Gladbach, Germany)]. This staining, as well as all other stainings described for other panels later in this article, were performed in the presence of Beriglobin (2 μg/100 μl; Sanofi-Aventis, Paris, France). Staining was stopped and erythrocytes lysed by adding 500 μl Buffer EL (Qiagen, Venlo, the Netherlands). After 15-min incubation at 4°C, samples were immediately analyzed on a MACSQuant (Miltenyi) or LSR II (BD Biosciences) flow cytometer without centrifugation. The cell trigger on the instruments was set to the CD45 channel. By analyzing a defined sample uptake volume, MACSQuant generated direct cell counts for the labeled populations. Cell counts measured on the LSR II were based on the use of BD TruCount tubes containing a defined number of fluorescent quantification beads. Counts of major leukocyte populations were used for calculations of any given cell subpopulation determined in other FACS panels.

Recent thymic emigrant panel. The naive/memory composition of the peripheral $CD8^+$ and $CD4^+$ T cell populations [including $CD4^+$ recent thymic emigrant (RTE)] were assessed on day 0. Staining of 5×10^6 PBMCs was here performed at 37°C using the following Ab mixture: anti-CD3 (OKT3), anti-CD45RA (RA3-6B2; both eBioscience), anti-CD8 (3B5; Invitrogen, Carlsbad, CA), anti-CD31 (AC128; Miltenyi), anti-CD4 (OKT4), anti-CD45RO (UCHL1), anti-CCR7 (G043H7), anti-CD27 (LG.3A10), and anti-CD62L (DREG-56; all Biolegend). Supplemental Fig. 1A illustrates the gating strategy for $CD4^+$ RTE. This panel included also an anti–HLA-A2 staining, which allowed discrimination of HLA-$A0201^+$ and HLA-$A0201^-$ individuals.

Innate cell panel. Innate cell subsets, such as monocytes and dendritic cells (DCs), were assessed by FACS on days 0, 4, 7, 10, 14, 17, 21, and 28. For this, 5×10^6 PBMCs of each donor were stained with a fluorescence-labeled mAb mixture containing anti-CD45 (2D1), anti-CD3 (SP34-2), anti-CD14 (M5E2), and anti-CD19 (HIB19; all BD Biosciences); anti-CD56 (HCD56), anti-CD16 (3G8), anti-BDCA1 (L1g1), and anti-HLA-DR (L243; all Biolegend); anti-CD11c (MJ4-27G12), anti-BDCA2 (AC144), and anti-CD141 (AD5-14H12; all Miltenyi), and anti-CD123 (6H6; eBioscience). Cells were washed once with PBS/BSA and analyzed on an LSR II flow cytometer. Before acquisition, DAPI was added at concentration of 0.01 μg/ml. The gating strategy for this panel is illustrated in Supplemental Fig. 1B. Absolute whole blood counts of these cell populations were calculated based on events acquired in the $CD14^{++}$ gate.

T cell activation panel. T cell subsets and their activation and proliferation status were analyzed at days 0, 2, 4, 7, 10, 14, 17, 21, and 28 after vaccination. For this, 5×10^6 PBMCs of each donor resuspended in 100 μl PBS/BSA were surface stained with the fluorescence-labeled mAb mixture containing anti-CD4 (OKT4), anti-CD8 (RPA-T8), anti-CCR7 (G043H7), anti-CD38 (HIT2), and anti–γδ-TCR (B1; all Biolegend), anti-CD45RA (HI 100; eBioscience), and anti–HLA-DR (G46-6), anti-CD14 (M5E2), and anti-CD19 (HIB19; all BD Biosciences) for 15 min at 37°C and in the dark. After 5 min of incubation, 1 μl L/D Red (Invitrogen) was supplemented to each sample. After incubation with surface Abs, cells were fixed and permeabilized with FOXP3 Fixation/Permeabilization Kit (eBioscience) according to manufacturer's protocol and stained intracellularly with anti-Helios (22F6; Biolegend), anti-FOXP3 (259D/C7), anti–Ki-67 (B56), and anti-CD3 (UCHT1; all BD Biosciences). Samples were acquired on an LSR II flow cytometer. A first scatter gate was set on the lymphocyte population; then $CD3^+$ cells were selected and $CD14^+$, $CD19^+$, and dead cells were excluded. γδ T cells were then selected and excluded from further analysis. The remaining cells were then assessed for their expression of CD4 and CD8. Out of the $CD4^+$ compartment, regulatory T cells were defined as $Helios^+/FOXP3^+$ and excluded from the following analysis of conventional $CD4^+$ T cells for phenotype and activation status, which was equally performed for $CD8^+$ T cells. Notably, assessment by activation/proliferation markers allows unequivocal identification of YF-specific T cells only in a narrow time window of the acute response, that is, between the release of the cells into the bloodstream until clearance of the pathogen ($CD8^+$ T cells: days ~10–21; $CD4^+$ T cells: days

~4–17) (15, 26–29). At all other days activated cells do not necessarily represent YF-specific T cells but rather, for example, steady-state turnover.

Assessment of specific CD4$^+$ T cells after YF vaccine stimulation. YF-specific CD4$^+$ T cells were measured after ex vivo stimulation of whole blood with YF vaccine (50 μl YF-vaccine = 1/3 vaccination dose) at study days 0, 2, 4, 7, 10, 14, 17, 21, and 28. Negative (unstimulated, supplementation of RPMI/AB medium) and positive [stimulated with 1.5 μg SEB/1.0 μg TSST1 (Sigma-Aldrich, Munich, Germany)] controls were performed simultaneously for each donor at all time points. For each stimulation, 1 ml freshly drawn heparinized blood was transferred into 12-ml round-bottom stimulation tubes (Greiner) and 1 μl purified anti-CD28 (BD Biosciences) was added. Tubes were then incubated for 2 h at 37°C under humid conditions and in 5% CO_2 atmosphere, capped permeable to air in a 45-degree position. After 2 h, brefeldin A (10 μg/ml; Sigma-Aldrich) was supplemented to each tube. After another 4 h of incubation, 100 μl 20 nM EDTA was added to stop the stimulation. Erythrocytes were lysed through addition of 10 ml Buffer EL (Qiagen) and intense vortexing. Lysis reaction was increased by 10-min incubation on ice. After centrifugation, supernatants were aspirated and the remaining cell pellets were then washed once again with 4 ml Buffer EL and centrifuged. After resuspension in PBS/BSA, cell pellets were transferred into FACS tubes and washed again with PBS/BSA. The surface staining was performed for 15 min at room temperature with the following Ab mixture: anti-CD8 (RPA-T8), anti-CD19 (HIB19), anti-CD14 (MφP9) (all BD Biosciences), and anti-CD4 (TT1, in-house DRFZ). After 5 min of incubation, 1 μl L/D Red (Invitrogen) was supplemented for live/dead discrimination. Staining was stopped by washing cells with PBS/BSA and fixating them by resuspension in 800 μl 1× BD FACS Lysing solution for 10 min at room temperature. Fixed cells were spun down, supernatants were discarded, and 300 μl 1× BD Perm 2 solution was added for permeabilization of samples. PBMCs were then washed twice with PBS/BSA and resuspended in 100 μl PBS/BSA for intracellular staining for 30 min at room temperature [Ab mixture: anti-CD40L (24–31), anti–IL-2 (MQ1-17H12), anti–IL-4 (MP4-25D2), anti–TNF-α (MAb11), anti–IFN-γ (B27), anti-RANKL (MIH24), anti–IL-17 (BL168; all Biolegend), and anti–IL-22 (22URTI) and anti-CD3 (OKT3; both eBioscience). Samples were measured on an LSR II flow cytometer. Analysis of cytokine production and activation markers was performed as illustrated in Supplemental Fig. 2A. All measured frequencies of cytokine- or activation marker–expressing cells were background subtracted by the matching unstimulated sample. For multidimensional assessment of cytokine expression and polyfunctionality, a SPICE analysis (30) was performed based on the expression of TNF-α, IFN-γ, IL-2, IL-4, IL-17, and RANKL. Averaged polyfunctionality of YF-specific CD40L$^+$ CD4$^+$ T cells, used in correlation analyses, was calculated based on polyfunctionality values from days 7 to 28 of each vaccinee. Geometric mean fluorescence intensity of IL-2 was analyzed for donors 15–28 (third round) from days 14 to 28 for all YF-specific CD4$^+$ T cell subsets being positive for IL-2. For this, functionality was based on TNF-α, IFN-γ, IL-4, IL-17, and RANKL expression. Assessment of vaccine-specific CD4$^+$ T cells at the late follow-up study day was conducted in a similar way with a modified FACS panel [surface staining: anti-CD8 (RPA-T8) and CCR7 (G043H7; both Biolegend); anti-CD19 (HIB19), anti-CD14 (MφP9), and anti-CD45RA (L48; all BD Biosciences); and CD4 (TT1, in-house DRFZ); intracellular staining: anti-CD40L (24–31), anti–IL-2 (MQ1-17H12), anti–IL-4 (MP4-25D2), anti–TNF-α (MAb11), anti–IFN-γ (B27), and anti–IL-17 (BL168; all Biolegend) and anti-CD3 (OKT3; eBioscience)].

Assessment of YF-specific CD8$^+$ T cells. YF-specific CD8$^+$ T cells were measured after ex vivo stimulation of PBMCs in HLA-A0201$^+$ donors (n = 10) at study days 0, 4, 7, 10, 14, 17, 21, and 28. At each day and for each HLA-A0201$^+$ donor the following stimulations were performed: negative control (unstimulated), positive control (SEB/TSST1 stimulated), and an NS4b 9mer peptide stimulation (LLWNGPMAV, 0.25 μg/μl in 50% DMSO/50% PBS). A total of 5 × 10^6 PBMCs were transferred into 12-ml round-bottom stimulation tubes in 500 μl RPMI/AB, and stimulation cocktails were added including Monensin A (BD Biosciences) and anti-CD107a (H4A3; Biolegend) Abs for all conditions. The total stimulation volume was 1 ml. Tubes were incubated for 2 h at 37°C, capped permeable to air, in a 45-degree position and under humid conditions and 5% CO_2 atmosphere. After 2 h, brefeldin A (10 μg/ml) was supplemented and stimulation was continued for another 4 h. To stop stimulation, we added 100 μl 20 nM EDTA. PBMCs were then washed once with 10 ml PBS/BSA and transferred into FACS tubes. The subsequent fixation, permeabilization, and staining procedure followed the CD4$^+$ T cell vaccine stimulation protocol using the following Ab cocktails: surface staining: anti-CD4 (RPA-T4; BD Biosciences) and anti-CD8 (RPA-T8; eBioscience); intracellular staining: anti-CD40L (24–31), anti–IL-2 (MQ1-17H12), anti–granzyme A (CB9), anti–IL-17(BL168), and anti–IFN-γ (B27; all Biolegend); anti–granzyme B (GB11; BD Biosciences); anti-CD3 (OKT3; eBioscience); and anti-Perforin (B-D48; Abcam). Samples were measured on an LSR II flow cytometer. Gating was performed by selection of CD3$^+$ and exclusion of doublets. CD4$^+$ and CD8$^+$ T cells were then selected according to their expression of CD4 and CD8 and then analyzed for their expression of the cytokines and activation markers included in the panel. All measured frequencies of cytokine- or activation marker–expressing cells were background subtracted by the matching unstimulated sample. Assessment of YF-specific CD8$^+$ T cells at the very late follow-up study day was conducted in a similar way with a modified FACS panel: surface staining: anti-CD4 (RPA-T4), anti-CD45RA (HI100), anti-CD8 (RPA-T8), and anti-CCR7 (G043H7; all Biolegend); anti-CD19 (HIB19) and anti-CD14 (MφP9; both BD Biosciences); intracellular staining: anti-CD40L (24–31), anti–IL-2 (MQ1-17H12), anti-CD3 (OKT3), anti–IL-17 (BL168), and anti–IFN-γ (B27; all Biolegend); anti–granzyme B (GB11; BD Biosciences); and anti-Perforin (B-D48; Abcam).

Data acquisition, analysis, and statistics

FACS data were acquired on LSR II by FACSDiva 6 and on MACSQuant by MACSQuantify Software. All FACS data were properly compensated using matching single-stain controls acquired 2–3 d before beginning of each study round. Instrument stability was monitored over the study course using BD Rainbow Calibration Particles. FACS data were analyzed with FlowJo 9.7.4. GraphPad Prism 5 was used for univariate statistical analysis. Principal component analysis (PCA) of innate immune cell types was conducted with R 3.02 (31) of 22 vaccinees. Z-scores for each population were calculated by subtracting the mean and dividing by the SD. Singular value decomposition was performed, and the first two principle components were displayed in a scatterplot. Median-separated response markers were used as a red/blue color overlay. Because the human immune response to primary live-viral vaccination in the elderly has never been investigated before, this study had an exploratory character with no initial assumptions regarding the effect sizes. Because a power test was therefore not possible, the size of the cohort was limited by available donors during the study time. No adjustment of the significance level for multiple testing was done to avoid an inappropriate increase of type II errors. The Shapiro test was used to test normal distribution of the data, which was rejected for most of the groups ($p < 0.05$). Unless stated otherwise, the two-sided Mann–Whitney U (MWW) test was used as a nonparametric test to compare differences in groups. Data were tested for homoscedasticity as a prerequisite for the Mann–Whitney U test with the Levene test ($p < 0.05$). In all group comparisons, medians and interquartile ranges were added. As indicated, Pearson's (R_P) or Spearman's (R_S) correlation was used to determine correlations. A p value ≤0.05 was required for significance in group and correlation analyses. Asterisks indicate levels of significance (*$p < 0.05$, **$p < 0.01$, ***$p < 0.001$). In most correlation plots a line indicating linear regression was added for better visualization.

Results

Elderly YF vaccinees show a late serum viremia

We immunized 11 young (median age: 26 y) and 12 elderly (median age: 60 y) YF-seronegative volunteers with live-attenuated YFV-17D. When YF viremia was assessed in the serum from days 0 to 10 by RT-PCR, all except 1 old vaccinee, but only 8 of 11 young vaccinees showed detectable viremia at least at one time point. Although absolute viral loads were comparable between both age groups at any day and at individual peaks (Supplemental Fig. 1C, 1D), the maximal viral burden was clearly delayed in several elderly subjects because two elderly subjects peaked at day 7 and two others even at day 10, whereas 7 of 8 young vaccinees had highest viral loads at day 4 or earlier. Hence late viral burden was significantly associated with age (Fig. 1A), which led us to hypothesize that antiviral effector functions are affected in elderly adults.

YF vaccination induces distinct kinetic patterns in peripheral leukocyte subsets

Being the base for our calculations of whole blood counts, we quantified major immune cell subsets in freshly drawn peripheral blood in the course of the infection. Interestingly, YF vaccination

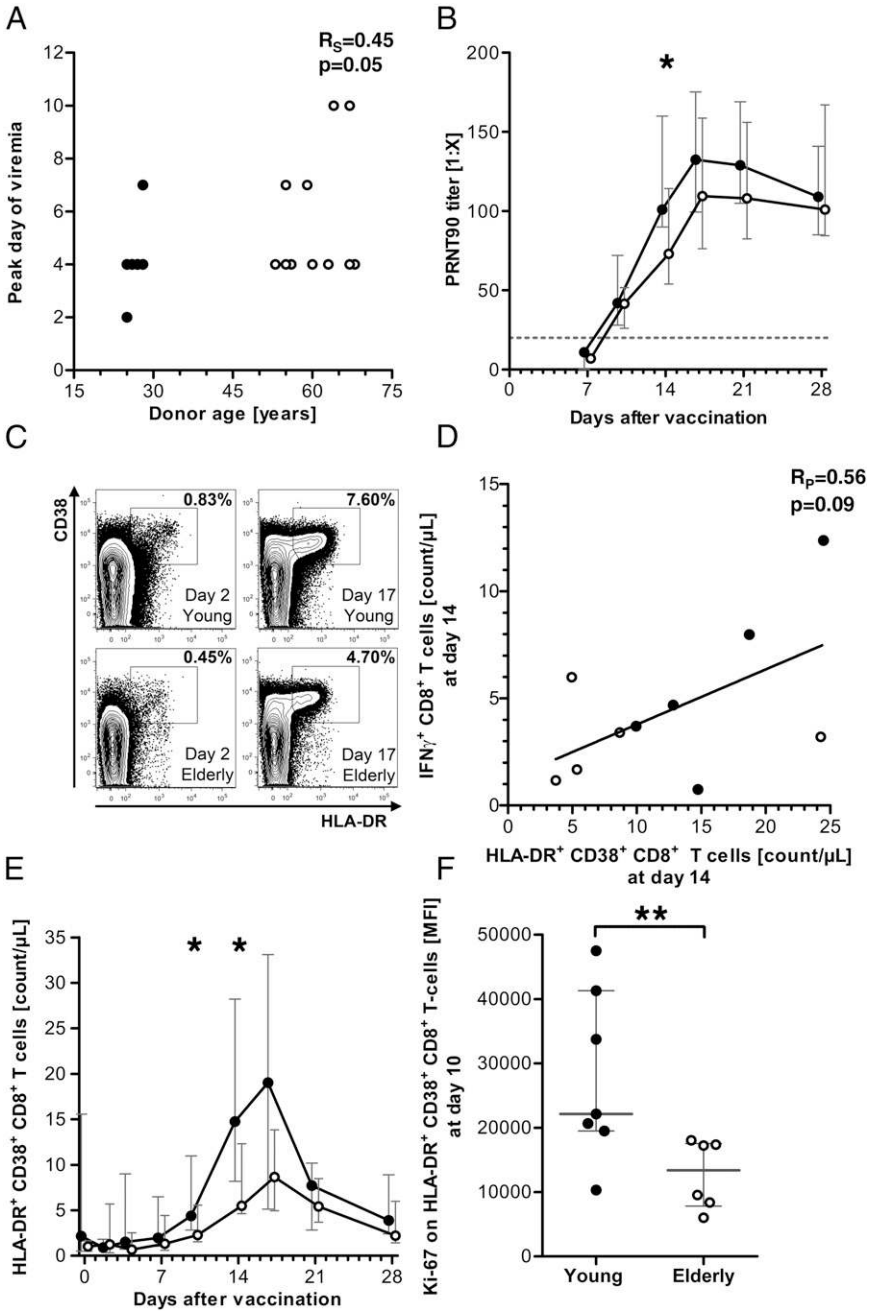

FIGURE 1. Elderly vaccinees show delayed YF viremia and compromised YF-specific humoral and $CD8^+$ T cell responses. (**A**) Individual peak days of viremia (day of maximum YF-genome equivalents per milliliter serum assessed by RT-PCR) versus donor's age (young: $n = 8$, elderly: $n = 11$). Individuals tested negatively for viremia at all time points ($n = 4/23$) were not included in this analysis. Spearman's rank correlation was used. (**B**) YF-neutralizing Ab titers assessed by PRNT90 (day 14: $p = 0.03$). Dashed line indicates the cutoff of the assay, $n = 23$. (**C**) Representative stainings of activated HLA-DR^+/$CD38^+$ $CD8^+$ T cells from a young and an elderly subject at days 2 and 17 after vaccination. (**D**) Correlation (Pearson) between numbers of activated HLA-DR^+/$CD38^+$ $CD8^+$ T cells at day 14 and IFN-γ^+ $CD8^+$ T cells at day 14 measured after YF-specific stimulation, $n = 10$. (**E**) Whole blood counts of activated HLA-DR^+/$CD38^+$ $CD8^+$ T cells in the course of the immune response to YFV-17D (day 10: $p = 0.04$; day 14: $p = 0.02$), $n = 23$. (**F**) Mean fluorescence intensity (MFI) of activated HLA-DR^+/$CD38^+$ $CD8^+$ T cells at day 10 ($p = 0.008$) of vaccinees of study round III, $n = 13$. (B, E, and F) Lines indicate the median with interquartile error bars. Two-sided MWW test was applied (A, B, and D–F). $^*p < 0.05$, $^{**}p < 0.01$, $^{***}p < 0.001$. ●, young; ○, elderly.

induced distinct kinetic patterns in different subsets (Supplemental Fig. 1E–I). Likewise observed after experimental vaccinia vaccination and accompanied there by local lymph node tenderness (32), we interpret these dynamics as migration of immune cells to and from secondary lymphoid tissue and/or the site of inflammation. Importantly, no significant age differences in whole blood counts of leukocytes, monocytes, B cells, and $CD4^+$ T cells were found before or at different days after vaccination, with the exception of $CD8^+$ T cells, which can be largely attributed to massively reduced naive $CD8^+$ T cell counts in the elderly, typical for an aged immune system (33, 34).

Humoral and cellular antiviral immune responses are compromised in the elderly

As an essential element of immune effector mechanisms in infection, we assessed YF-neutralizing Abs by PRNT90 and observed transiently reduced YF-neutralizing Ab titers (day 14: $p = 0.03$) in elderly vaccinees (Fig. 1B), although by day 28 both age groups reached comparable levels. Complementing humoral anti-YF immunity (35), we furthermore monitored YF-specific $CD8^+$ T cells over the course of the immune response, using the activation markers CD38 and HLA-DR (Fig. 1C). Coexpression of both markers can be used to track acutely induced, YF-specific $CD8^+$ T cells after vaccination (16), which we validated in all HLA-$A0201^+$ study participants ($n = 10$) by YF-specific peptide stimulation and intracellular cytokine staining (Fig. 1D). We detected a strong increase of acutely induced $CD38^+$/HLA-DR^+ YF-specific $CD8^+$ T cells at days 14 and 17, which returned to steady-state levels by day 28 (Fig. 1E). Importantly, the magnitude of the YF-specific $CD8^+$ T cell response was significantly reduced in older vaccinees (day 10: $p = 0.04$; day 14: $p = 0.02$) and, in addition, cells showed reduced proliferation, indicated by a lower Ki-67 mean fluorescence intensity, for example, at day 10 in the elderly cohort (Fig. 1F). Thus, both the acute humoral and the

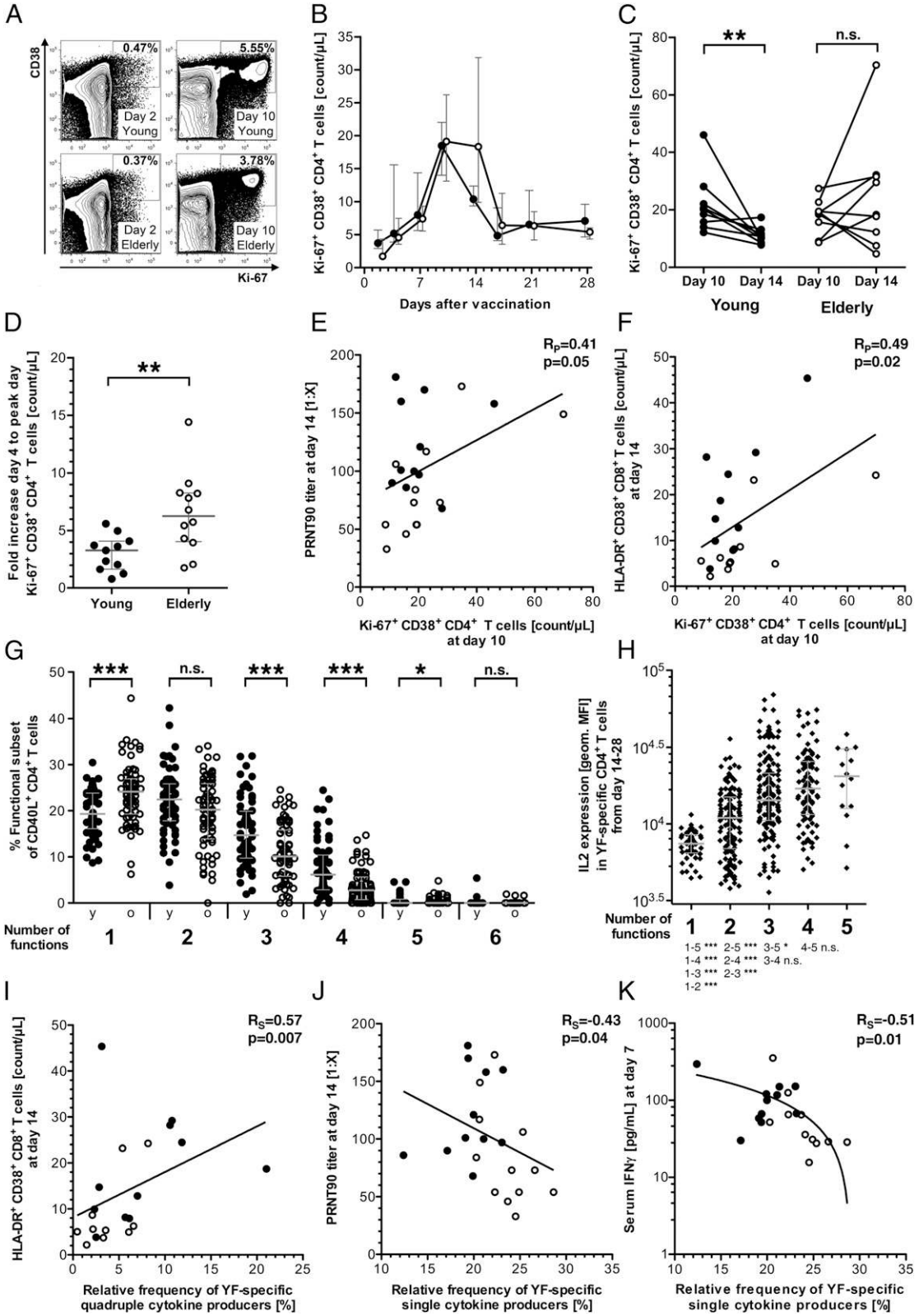

FIGURE 2. The YF-specific CD4$^+$ T cell response is quantitatively and qualitatively altered in the elderly. (**A**) Representative stainings of activated/proliferating Ki-67$^+$/CD38$^+$ CD4$^+$ T cells of the same subjects as in Fig. 1C at days 2 and 10 after vaccination. (**B**) Whole blood counts of activated/proliferating Ki-67$^+$/CD38$^+$ CD4$^+$ T cells in the course of the immune response to YFV-17D; $n = 23$. (**C**) Individual changes in counts of Ki-67$^+$/CD38$^+$ CD4$^+$ T cells between days 10 and 14 of both age groups. A Wilcoxon signed-rank test was performed (young: $p = 0.008$). (**D**) Total vaccine-induced (Ki-67$^+$/CD38$^+$) CD4$^+$ T cell expansion (fold change of counts at day 4 to individual peak days) ($p = 0.006$), $n = 23$. (**E** and **F**) Numbers of Ki-67$^+$/CD38$^+$ CD4$^+$ T cells at day 10 positively correlate (Pearson) with (E) YF-neutralizing Ab titers at day 14 ($n = 23$) and (F) with numbers of HLA-DR$^+$/CD38$^+$ CD8$^+$ T cells at day 14 ($n = 21$). Similar positive correlations were found for days 4 and 7 of Ki-67$^+$/CD38$^+$ CD4$^+$ T cells. (**G**) Age comparison of single functionality/polyfunctionality of YF-specific CD40L$^+$ CD4$^+$ T cells. Vaccine stimulation data from days 7 to 28 are superimposed. Number of functions is calculated on expression of TNF-α, IFN-γ, IL-2, IL-4, IL-17, and RANKL. (1 function: $p = 0.0002$; 3 functions: $p = 0.0006$; 4 functions: (*Figure legend continues*)

acute $CD8^+$ T cell response were clearly affected by aging, which could have negative consequences for clearance of YF virus in elderly humans.

Quantitative and qualitative alterations in YF-specific $CD4^+$ T cells in elderly adults

Because humoral and cellular antiviral defense mechanisms are orchestrated by $CD4^+$ Th cells, we also studied YF-induced $CD4^+$ T cells. Tracking them by coexpression of CD38 and Ki-67 (Fig. 2A) (29) demonstrated a strong increase in their numbers in both age groups (Fig. 2B). Interestingly, in almost all young vaccinees, the highest number of YF-activated $CD4^+$ T cells was reached already at day 10 (Fig. 2C), whereas in ~50% of the elderly subjects, YF-activated $CD4^+$ T cells continued to increase until day 14. Consequently, the calculated total expansion to individual response peaks was significantly higher ($p = 0.006$) in the old cohort (Fig. 2D). Remarkably, although not depending significantly on age by itself, YF-specific $CD4^+$ T cell numbers in the early expansion phase (days 4/7/10) correlated with YF-neutralizing Abs and YF-specific $CD8^+$ T cell numbers at day 14 (Fig. 2E, 2F), suggesting that robust early YF-specific $CD4^+$ T cell responses indeed positively affected both antiviral effector mechanisms.

We furthermore assessed the functional quality of YF-specific $CD40L^+$ $CD4^+$ T cells by analyzing cytokine production after whole blood stimulation with YF vaccine (Supplemental Fig. 2A). In both age groups, the YF-specific $CD4^+$ T cell response was dominated by TNF-α, IL-2, and IFN-γ expression, whereas smaller fractions expressed IL-4, IL-17, and/or IL-22 (Supplemental Fig. 2B–G). Interestingly, polyfunctionality, proposed to be associated with protective immunity against various pathogens (36, 37), was significantly decreased in YF-specific $CD40L^+$ $CD4^+$ T cells of aged vaccinees (three to five functions) (Fig. 2G). Instead, the elderly subjects possessed higher frequencies of single-cytokine–producing, YF-specific $CD4^+$ T cells throughout the response. Moreover, and in accordance with other reports (38, 39), we could observe that increased averaged polyfunctionality was associated with higher cytokine expression, for example, of IL-2 and IFN-γ (Fig. 2H and data not shown) on a per-cell basis. Intriguingly, averaged YF-specific $CD4^+$ polyfunctionality positively correlated with numbers of YF-specific $CD8^+$ T cells at day 14 (Fig. 2I), whereas single functionality negatively correlated with YF-neutralizing Abs at day 14 (Fig. 2J). Moreover, we could also observe a relation between serum IFN-γ levels, significantly reduced in the elderly subjects at day 7 after vaccination (Supplemental Fig. 2I), and $CD4^+$ polyfunctionality (Fig. 2K). Thus, our data suggest that besides quantitative differences, also qualitative alterations occur in acutely induced YF-specific $CD4^+$ T cells in elderly vaccinees, negatively affecting systemic cellular and humoral antiviral effector responses.

Reduced initial naive $CD8^+$ T cell numbers and thymic output in elderly adults are associated with weak T cell responses

Next, we tried to explore immune signatures before vaccination that can be linked to the altered humoral and cellular immune responses observed in elderly adults. From animal experiments, it has been suggested that the diversity of the immune receptor repertoire critically governs primary immune responses against pathogens (11–13).

Therefore, we assessed the thymic activity before vaccination as characterized by the quantity of naive $CD8^+$ T cells and $CD4^+$ RTEs. We observed significantly ($p = 0.0002$) lower numbers of naive $CD8^+$ T cells in the elderly subjects on the day of vaccination (Fig. 3A), which significantly correlated with the YF-specific $CD8^+$ T cell response at day 14 (Fig. 3B). In a similar manner, significantly ($p = 0.005$) reduced prevaccination numbers and frequencies of $CD4^+$ RTEs (Fig. 3C, 3D), which can be identified by their expression of CD31 (Supplemental Fig. 1A) (40) and which represent a surrogate marker for human thymic activity (41), significantly correlated with early YF-specific $CD4^+$ T cell responses at days 4, 7, and 10 (Fig. 3E–G), with the qualitative functionality of YF-specific $CD4^+$ T cells (Fig. 3H, 3I) and also with the YF-specific $CD8^+$ T cell response at day 14 (Fig. 3J), whereas the age-related prolonged $CD4^+$ T cell expansion was negatively associated with $CD4^+$ RTEs (Fig. 3K). Collectively, our data indicates that deteriorated human thymic activity as observed in elderly individuals affects both YF-specific $CD4^+$ and $CD8^+$ T cell immunity in quantitative and in qualitative aspects.

Reduced early DC responses in the elderly are associated with decreased YF-specific adaptive immunity

Because induction of innate immunity by YF vaccination has been shown to critically influence elicitation of subsequent effector responses (18, 42, 43), we assessed absolute numbers of seven circulating innate cell types (Supplemental Fig. 1B) and evaluated them on the peak of innate immunity at day 4 by PCA. YF vaccinees could be segregated into two large clusters following largely the age criterion with only one old and three young misclassified individuals (two-tailed Fisher's test: $p = 0.007$) (Fig. 4A). Two of the most determining parameters were numbers of plasmacytoid DCs (pDCs) and type I $CD11c^+$ myeloid DCs (mDC1), which were significantly decreased in elderly subjects in the innate response phase (Fig. 4B, 4C). Interestingly, the pDC peak on day 4 coincided with the occurrence of mild adverse reactions to vaccination such as fever, myalgia, and erythema. Grouping vaccinees according to these symptoms revealed a significant ($p = 0.005$) difference in pDC numbers at day 4; that is, increased numbers of pDCs were characteristic for vaccinees reporting any symptoms (Supplemental Fig. 3A, 3B). Hence mild adverse events reflect a pronounced induction of innate immunity, especially in the young, that is indicative of a competent immune activation. In fact, we found significant positive correlations between pDC and mDC1 numbers at day 4 and YF-specific $CD8^+$ T cell numbers at day 14 (Fig. 4D, 4E). Moreover, numbers of mDC1 at day 4 positively correlated with YF-specific $CD4^+$ T cell numbers in the early expansion phase at days 4/7 (Supplemental Fig. 3C, 3D), whereas pDCs at day 4 seemed to promote $CD4^+$ polyfunctionality (Supplemental Fig. 3E, 3F). Consistently, we could visualize these associations in our PCA of early innate immunity when

$p < 0.0001$; 5 functions: $p = 0.02$) $n = 6*23 = 138$. (**H**) Geometric mean fluorescence intensity of IL-2 in YF-specific $CD40L^+$ $CD4^+$ T cell subsets grouped by the number of functions they exert. Vaccinees 15–28 (third round) at days 14–28 are superimposed. Each symbol represents one subset of one donor at 1 d. (**I**) Correlation (Spearman) between percentage of quadruple functionality and numbers of activated $HLA\text{-}DR^+/CD38^+$ $CD8^+$ T cells at day 14 after vaccination. A similar correlation can be found for quintuple functionality. $n = 23$. (**J** and **K**) Negative correlations (Spearman) between frequency of single functionality and (J) YF-neutralizing titers at day 14 ($n = 21$) and (K) serum IFN-γ levels at day 7 after vaccination ($n = 22$). (B, D, G, and H) Lines indicate the median with interquartile error bars. Two-sided MWW test was applied (B–G, I, J, and K). $*p < 0.05$, $**p < 0.01$, $***p < 0.001$. ●, young; ○, elderly.

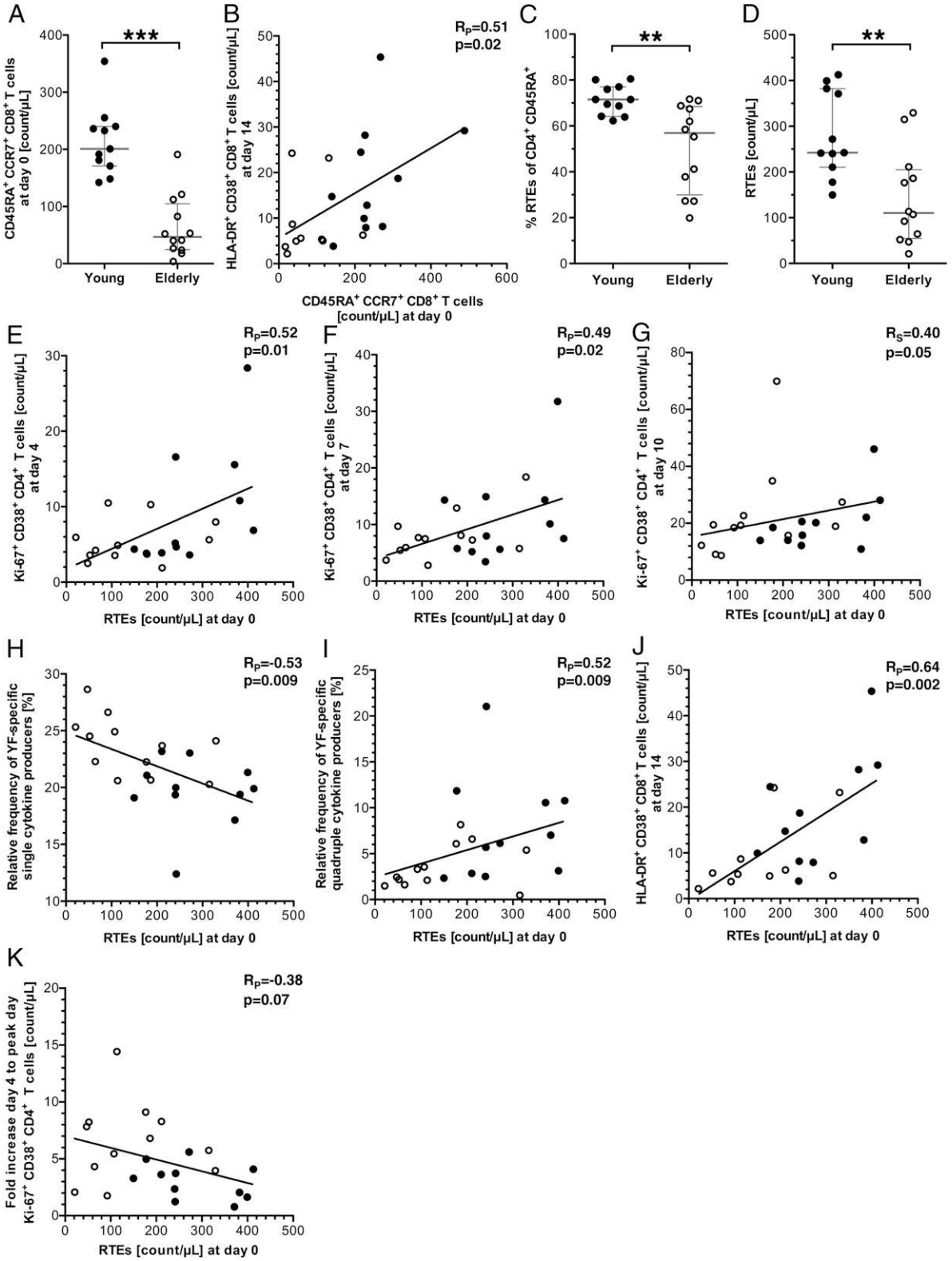

FIGURE 3. Quantity and quality of YF-specific T cell responses are associated with prevaccination numbers of naive $CD8^+$ T cells and $CD4^+$ RTEs. (**A**) Whole blood counts of naive $CD45RA^+/CCR7^+$ $CD8^+$ T cells at day 0 ($p = 0.0002$), $n = 23$. (**B**) Correlation (Pearson) between naive $CD8^+$ T cell counts at baseline and counts of activated, YF-specific $HLA\text{-}DR^+/CD38^+$ $CD8^+$ T cells at day 14, $n = 21$. (**C**) Percentage and (**D**) whole blood counts of $CD4^+$ RTE ($CD45RA^+/CCR7^+/CD27^+/CD31^+$ $CD4^+$ T cells) at day 0 of young and elderly vaccinees (percentage: $p = 0.004$; count $p = 0.005$), $n = 23$. (**E**–**G**) Positive correlations (Pearson or Spearman) between numbers of $CD4^+$ RTEs at day 0 and numbers of activated $Ki\text{-}67^+/CD38^+$ $CD4^+$ T cells at days 4, 7, and 10 after vaccination, $n = 23$. (**H** and **I**) Correlations (Pearson) between numbers of RTEs at day 0 and qualitative YF-specific single and quadruple $CD4^+$ functionality, $n = 23$. (**J**) Positive correlation (Pearson) between numbers of RTEs at day 0 and numbers of activated $HLA\text{-}DR^+/CD38^+$ $CD8^+$ T cells at day 14 after vaccination, $n = 21$. (**K**) Negative correlation (Pearson) between numbers of RTEs at day 0 and total vaccine-induced ($Ki\text{-}67^+/CD38^+$) $CD4^+$ T cell expansion, $n = 23$. (A, C, and D) Lines indicate the median with interquartile error bars. (A–K) Two-sided MWW test was applied. $^{**}p < 0.01$, $^{***}p < 0.001$. ●, young; ○, elderly.

we overlaid median-segregated, YF-specific response signatures (Fig. 4F, 4G, Supplemental Fig. 3G). Notably, although these response signatures as expected largely assigned to both age clusters, age-misclassified individuals often exhibited adaptive responses closely resembling those of circumjacent subjects, underlining the importance of the individual innate constitution on subsequent primary adaptive immunity beyond the level of pure age discrimination. Altogether, high numbers of pDCs and mDC1, predominantly observed in young individuals, seem to support competent YF-specific $CD4^+$ and $CD8^+$ T cell responses.

Chronic viral infections do not affect primary YF-specific immune responses

It has been emphasized that persistent infections such as CMV and EBV infection provoke accelerated immunosenescence and are therefore causative for reduced vaccination efficiency in elderly adults (8, 44–46). All vaccinees in our study had EBV-specific IgG Abs with titers not differing between age groups (Fig. 5A). CMV-specific IgG Abs were found in 58% old and 45% young vaccinees, and titers were also equal in both age groups (Fig. 5B). Importantly, neither EBV nor CMV immune status had an impact on

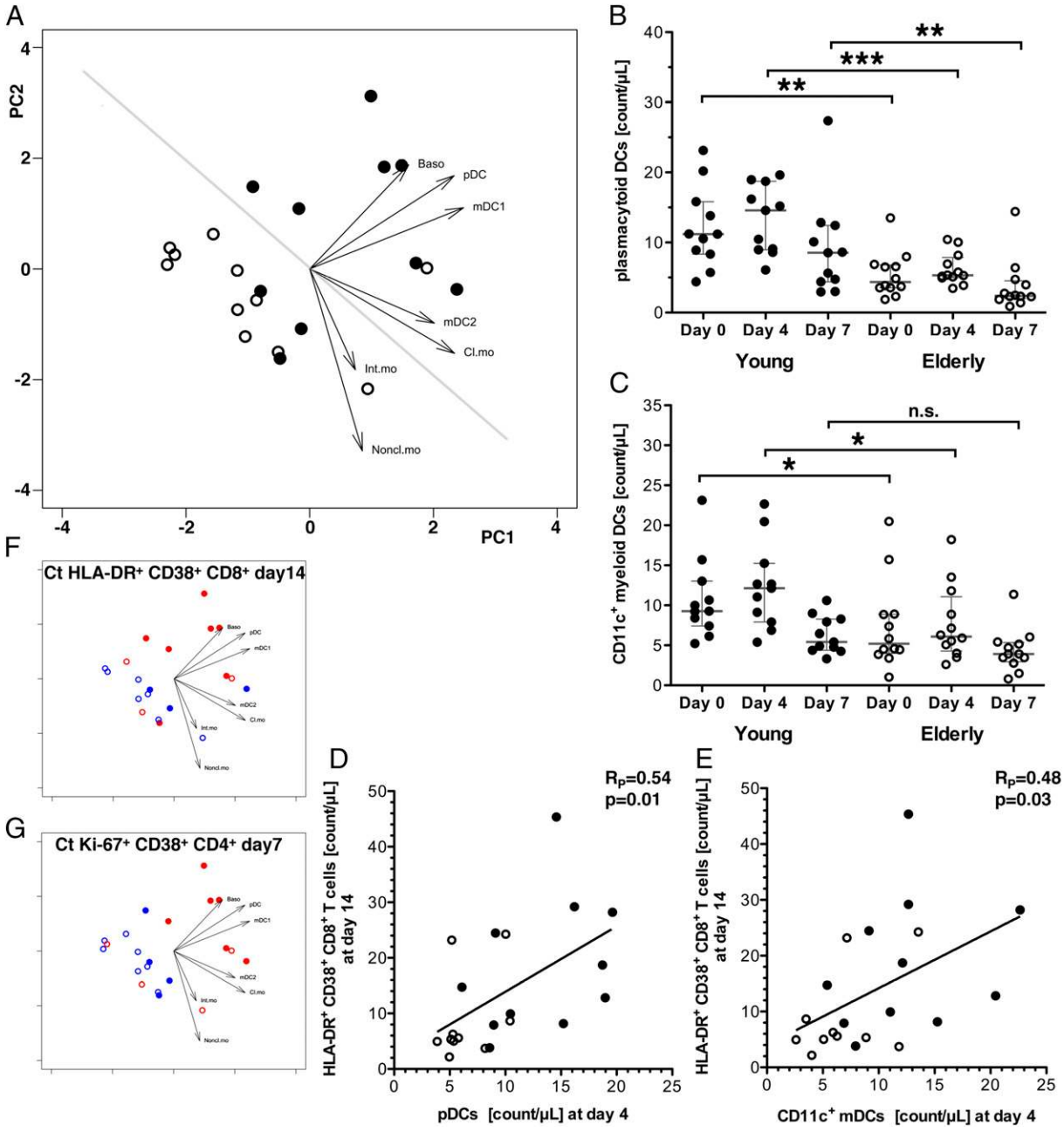

FIGURE 4. Early innate constitution is altered in the elderly and associated with YF-specific cellular responses. (**A**) PCA of innate immunity at day 4 based on whole blood numbers of seven major innate cell subsets. Vector arrows indicate contribution of innate components on PCA (2-fold magnified), n = 22. (**B** and **C**) Numbers of (B) pDCs or (C) mDC1 in peripheral blood at days 0, 4, and 7 after vaccination (pDCs: day 0, $p = 0.004$; day 4, $p = 0.0006$; day 7, $p = 0.005$; mDC1: day 0, $p = 0.05$; day 4, $p = 0.03$), n = 23. (**D** and **E**) Positive correlations (Pearson) between numbers of (D) pDCs or (E) mDC1 at day 4 and numbers of activated $HLA\text{-}DR^+/CD38^+$ $CD8^+$ T cells at day 14 after vaccination, n = 21. (**F** and **G**) Color overlay of median separated values of (F) activated $HLA\text{-}DR^+/CD38^+$ $CD8^+$ T cells at day 14 or (G) activated $Ki\text{-}67^+/CD38^+$ $CD4^+$ T cells at day 7 on innate PCA at day 4, n = 22. Red: values > median; blue: values < median. (B and C) Lines indicate the median with interquartile error bars. (A–G) Two-sided MWW test was applied. $^*p < 0.05$, $^{**}p < 0.01$, $^{***}p < 0.001$. ●, young; ○, elderly.

YF-induced humoral or cellular immunity (Fig. 5C, Supplemental Fig. 4A–E). In line with this, EBV and CMV status could not be linked to initial naive T cell numbers or thymic output (Supplemental Fig. 4F, 4G, 4I, 4J), although general effector T cell differentiation was affected (Supplemental Fig. 4H, 4K).

Long-lasting YF-specific immunity is dependent on initial and early immune parameters

Finally, we assessed long-term YF-specific immunity in 8 young and 11 old reinvited study participants up to 3 y after YF vaccination. As shown in Fig. 6A–C, protective YF-neutralizing Abs and YF-specific $CD8^+$ and $CD4^+$ T cells were preserved in all vaccinees. However, long-term numbers of YF-specific IFN-γ^+ $CD40L^+$ $CD4^+$ T cells were significantly reduced in the elderly subjects (Fig. 6D), which was also reflected in reduced polyfunctionality in their YF-specific $CD4^+$ compartment (Fig. 6E). Interestingly, strength of long-term YF-specific T cell immunity was strongly determined by the acute T cell response, because high numbers of YF-specific $CD4^+$ and $CD8^+$ T cells during the acute phase (e.g., at day 17) led to increased numbers of these cells in long-term immunity (Fig. 6F, 6G). In line with this, prevaccination $CD4^+$ RTE numbers and early pDC numbers were also strongly associated with long-term YF-specific $CD4^+$ T cell immunity (Fig. 6H, 6I), indicating that these immune signatures are key factors for the induction of a long-lasting T cell memory as well.

Discussion

In this study, we demonstrate that immunological aging affects the primary response to YF vaccination at multiple levels. Several of our elderly vaccinees showed late serum viremia at days 7 or 10, confirming similar observations by Roukens et al. (47). Late serum viremia has been furthermore reported in a 64-y-old vaccinee who experienced YF-SAE (48) and in aged mice after primary influenza virus infection (49). Because YF serum viremia usually occurs earlier between days 2 and 6 (24, 28, 50), we propose that late viremia in the elderly is a consequence of impaired viral clearance due to diminished antiviral immune effector mechanisms. Indeed, and in line with a previous report (47), we observed transiently reduced YF-neutralizing Ab titers in elderly vaccinees, which could probably be attributed to the delayed production of YF-specific IgM Abs (data not shown). In addition, YF-specific $CD8^+$ T cells, known to complement humoral anti-YF immunity (35), were clearly reduced in numbers and in the acute phase of the response in the aged cohort, confirming similar observations from various aged animal models (49, 51–53). Although we could demonstrate an age-related proliferative defect of these cells in the acute phase as it has been seen also in aged mice after *Listeria monocytogenes* infection (54), other functional properties such as the specific $CD8^+$ cytotoxicity and cytokine expression remain to be addressed by future studies. Interestingly, studies comparing $CD8^+$ T cell responses in young and old individuals postinfection with West Nile flavivirus (WNV) could not find any age deficiencies in the response magnitude (55, 56) and in the functional properties (57), contrasting our results, although both viruses are closely related to each other. However, in the WNV studies, specific $CD8^+$ T cells were measured in the early memory phase, for example, 3–4 mo after onset of symptoms, whereas our data refer to specific cells in the well-defined acute response phase around day 14 after experimental infection. This difference in the analysis window might be one explanation for the opposing results between the WNV studies and our YF study, especially when considering our YF-specific long-term memory $CD8^+$ T cell data, which indeed did not show any age difference. We furthermore identified quantitative and qualitative age differences in the YF-specific $CD4^+$ T cell response. Both age groups started to mount on average comparable early acute Ki-67^+ $CD38^+$ $CD4^+$ T cell responses, but interestingly while the response in nearly all young adults was culminating already on day 10, in about half of the aged vaccinees $CD4^+$ T cells continued to expand until day 14, leading to a significantly enhanced total $CD4^+$ expansion in the aged group, which is comparable with data from aged macaques after primary WNV infection and from influenza-infected aged mice (5, 58). Although the early expansion of YF-specific $CD4^+$ T cells seemed to be key for better humoral and $CD8^+$ T cell immunity, age-associated increased late $CD4^+$ expansion on day 14 hints for a prolonged or exaggerated response, which might represent a countermeasure to still adequately fight back a viral attack in an immunosenescent situation with a weakened virus defense. In addition to that, YF-specific $CD4^+$ T cells in elderly vaccinees were significantly less polyfunctional and conversely more monofunctional than their counterparts in young individuals. Known to be a very good correlate for improved pathogen control and better vaccination responses (36, 37), $CD4^+$ polyfunctionality in our study indeed could be related to higher serum IFN-γ levels and better neutralizing Ab titers and $CD8^+$ T cell responses. Although we verified our assessment of vaccine-induced T cell activation by Ag-specific ex vivo stimulation, we cannot completely rule out that we measured some $CD4^+$ and $CD8^+$ bystander activation in our study. However, published data from others and us show that at least in young vaccinees nonrelated T cell specificities

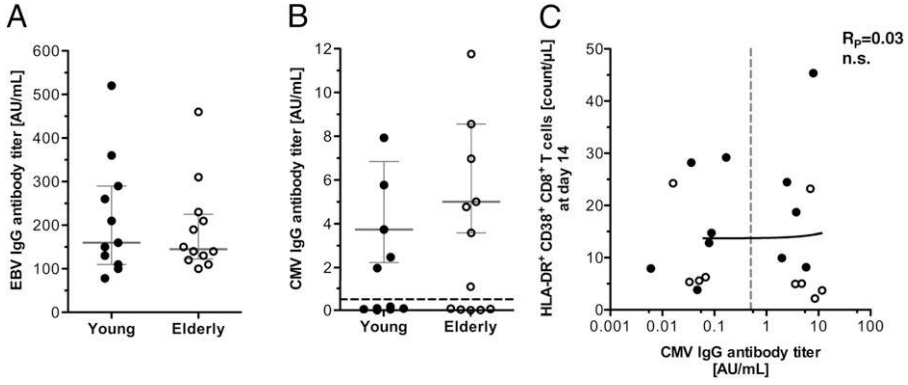

FIGURE 5. Influence of CMV and EBV sero status on YF-specific immunity. (**A**) EBV and (**B**) CMV IgG sero status of young and elderly vaccinees. Values below dashed line indicate negative sero status. No significant difference between both age cohorts was observed, $n = 23$. (**C**) No association (Pearson) between CMV IgG sero status and activated HLA-DR^+/$CD38^+$ $CD8^+$ T cells at day 14, $n = 21$. See also Supplemental Fig. 4. (A and B) Lines indicate the median with interquartile error bars. (A–C) Two-sided MWW test was applied. ●, young; ○, elderly.

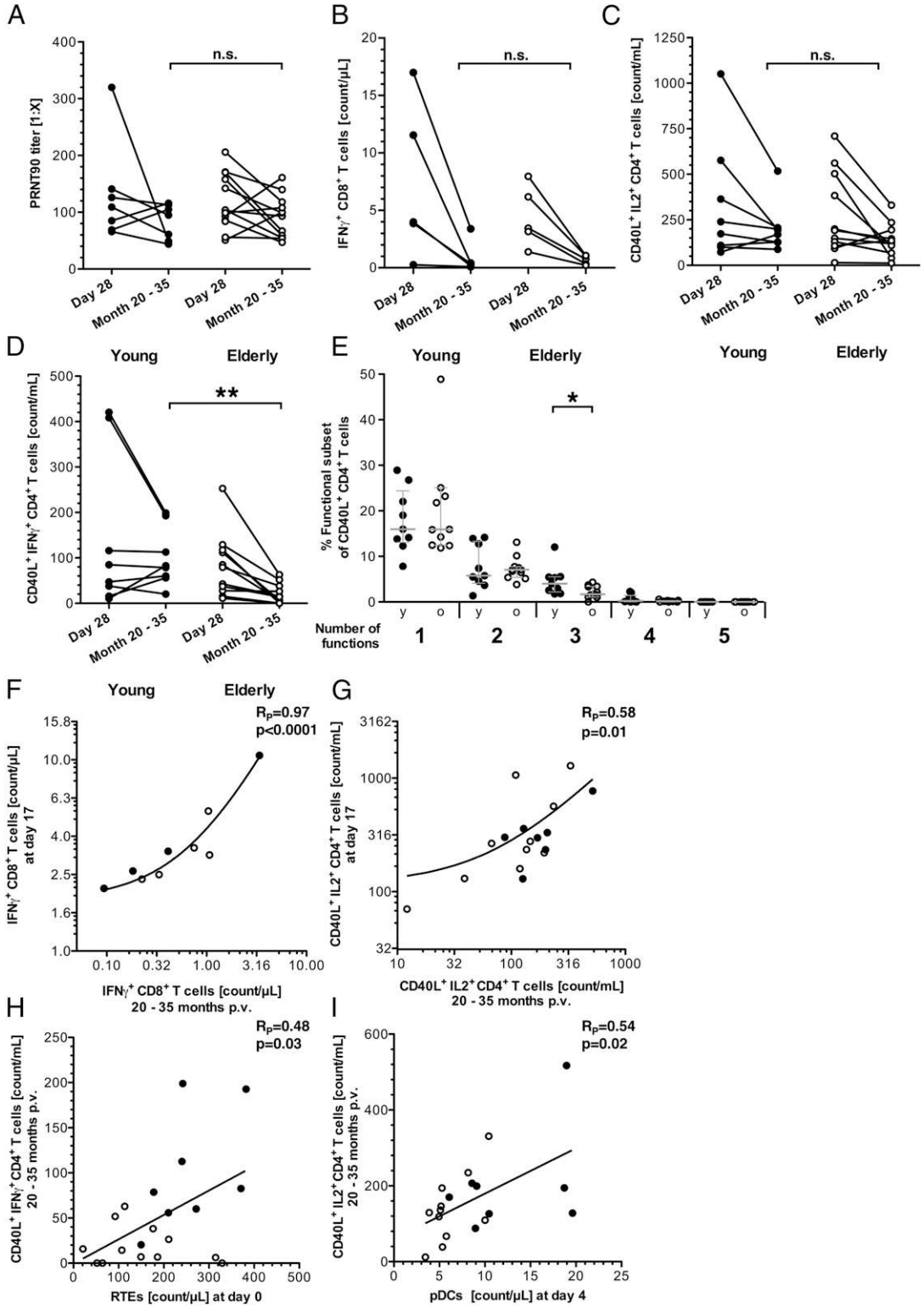

FIGURE 6. Long-term YF-specific immunity. (**A**) Individual changes in YF-neutralizing titers from day 28 to 20–35 mo after vaccination in both age groups, $n = 19$. (**B**) Individual changes of YF-specific IFN-γ$^+$ CD8$^+$ T cells from day 28 to 20–35 mo after vaccination in both age groups (HLA-A0201$^+$ donors only, $n = 9$). (**C**) Individual changes of YF-specific CD40L$^+$ IL-2$^+$ CD4$^+$ T cells from day 28 to 20–35 mo after vaccination in both age groups, $n = 19$. (**D**) Individual changes of YF-specific CD40L$^+$ IFN-γ$^+$ CD4$^+$ T cells from day 28 to 20–35 mo after vaccination in both age groups ($p = 0.002$), $n = 19$. (**E**) Age comparison of single functionality/polyfunctionality of YF-specific CD40L$^+$ CD4$^+$ T cells 20–35 mo after vaccination. Number of functions is calculated on expression of TNF-α, IFN-γ, IL-2, IL-4, and IL-17. (3 fcts: $p = 0.02$.) $n = 19$. Lines indicate the median with interquartile error bars. (**F**) Strong correlation (Pearson) between numbers of YF-specific IFN-γ$^+$ CD8$^+$ T cells at day 17 and 20–35 mo after vaccination, $n = 9$. Similar correlations were found also for days 21 and 28. (**G**) Correlation (Pearson) between numbers of YF-specific CD40L$^+$ IL-2$^+$ CD4$^+$ T cells at day 17 and 20–35 mo after vaccination, $n = 19$. Similar correlations were found also for days 7–28. (**H**) Correlation (Pearson) between initial numbers of CD4$^+$ RTEs and long-term numbers of CD40L$^+$ IFN-γ$^+$ CD4$^+$ T cells, $n = 20$. (**I**) Correlation (Pearson) between numbers of pDCs at day 4 and long-term numbers of CD40L$^+$ IL-2$^+$ CD4$^+$ T cells, $n = 20$. (A–E) Two-sided MWW test was applied. *$p < 0.05$, **$p < 0.01$. ●, young; ○, elderly.

transiently increase in peripheral numbers but do not show signs of activation (15, 16). Importantly, we can rule out for our study that reactive T cell counts simply reflect the total cell counts, because underlying total leukocyte counts were not affected by age.

Having identified prominent age differences in the YF-specific acute adaptive immune response, we searched for associated prevaccination and early immune signatures. Importantly, we discovered that limited availability of naive $CD8^+$ T cells and $CD4^+$ RTEs before vaccination adversely affected the specific immune response to the viral neoantigen, especially in the elderly. Interestingly, although not apparently depending on chronological age itself, Ki-67^+ $CD38^+$ $CD4^+$ T cells in the early expansion phase (days 4–10) correlated well with prevaccination $CD4^+$ RTE status, demonstrating that thymic activity much better reflects biological aging than chronological aging. Higher $CD4^+$ RTE numbers furthermore seemed to promote $CD4^+$ polyfunctionality and $CD8^+$ T cell responsiveness; in contrast, when initial supply with $CD4^+$ RTE was limited, $CD4^+$ expansion (day 14) was more likely to be improperly prolonged and/or exaggerated. Altogether, our in vivo findings confirm for the first time, to our knowledge, the long-suspected influence of thymic function on primary, Ag-specific adaptive human T cell immunity and also provide a plausible explanation for the high incidence of YF-SAE in thymectomized vaccinees (21).

In addition, we report that induction of YF-specific adaptive immunity in the elderly is critically affected by constrictions in the aged innate immune system. As previously shown, innate immunity induced by YF vaccination is generally important for the vaccine response outcome (18, 42, 43). In this article, we showed that we could classify vaccinees according to their age by multivariate analysis of major innate cell types. This age discrimination was most prominent in the activated state on day 4 but could be observed also at baseline prior vaccination (data not shown). Most determining factors were high peripheral numbers of pDCs and mDC1 in the young cohort, whereas the elderly subjects showed by trend increased numbers of $CD14^+/CD16^+$ nonclassical monocytes confirming data from literature (59–61). It is very likely that the reduced incidence of mild adverse reactions, such as fever, headache, or myalgia observed in particular in our elderly cohort, but also in two other large YF studies (62, 63), is a result of low numbers of proinflammatory pDCs (64, 65) probably in combination with age-related functional defects (60, 66, 67) observed also in WNV-infected DCs in aged individuals (68). Therefore, low DC numbers early postinfection reflect a state of poor innate immune activation, which affects adaptive immunity, as indicated by low early pDC and mDC1 numbers strongly linked to weak YF-specific $CD4^+$ and $CD8^+$ T cell responses and reduced $CD4^+$ polyfunctionality.

We additionally investigated the influence of chronic CMV and EBV infections in our study and, as expected, observed a clear impact on total baseline numbers of effector T cells. However, we could not prove any influence of CMV/EBV infections on the YF-specific immune response or on initial numbers of $CD4^+$ RTE and naive $CD8^+$ T cells. Given the size of our study, we cannot completely rule out any influence of persistent viral infections on the vaccine response outcome as it has been described in aged mice models (69, 70). However, it seems that the impact of these persistent infections is rather low in comparison with other signatures we have found.

Finally, we report for the first time, to our knowledge, a comprehensive long-term tracking of young and old YF vaccinees. The data we have obtained demonstrated that both age groups still maintained protective YF-neutralizing Abs and YF-specific T cells up to 3 y after vaccination. However, we could also observe an altered YF-specific $CD4^+$ T cell memory in our elderly vaccinees. In light of a recent World Health Organization announcement suggesting that YF booster vaccinations are dispensable (71), the altered YF-specific $CD4^+$ T cell memory in our elderly vaccinees raises the possibility that this recommendation may not be generally applicable to all elderly subjects. Another interesting finding is the close association of long-term YF-specific T cell immunity with prevaccination $CD4^+$ RTE and early pDC numbers, which demonstrates again that these initial and early immune signatures are key factors for the induction of a proficient and long-lasting T cell memory.

Collectively, our study demonstrates that the primary immune response to a living virus is compromised in elderly humans on manifold levels, with naive T cells and DCs representing the most restrictive elements. The limited availability of these two cell types in the elderly has been well documented and potentially explains the generally high susceptibility of the elderly to infections by newly emerging pathogens, such as WNV (72) or severe acute respiratory syndrome coronavirus (73). Although our study was restricted to relatively young elderly participants because of ethical reasons, we could clearly observe age-related deficiencies in response to vaccination, indicating that the ability of the immune systems to respond to neopathogens is already compromised at an age of around 60 y. The immune alterations observed in our elderly vaccinees were harmless, resulting in only mild changes of adaptive immunity and accordingly slightly increased viremia. However, at more advanced age, the observed impairments might be more pronounced and a resulting prolonged viremia (48) accompanied by increased immune activation might well be a major mechanisms for life-threatening YF-SAE occasionally observed in old vaccinees (20). Our results provide a rational to establish simple prevaccination risk assessment strategies in the elderly or immune-compromised individuals, who could benefit from analysis of critical immunological signatures such as $CD4^+$ RTEs and peripheral DCs.

Although the response to YF vaccination was reduced in the elderly cohort, protective immunity was eventually achieved in all vaccinees, which render YF-based vaccination strategies a powerful tool for immune specificities difficult to induce in aged individuals (74). Moreover, future studies will take advantage of YF vaccination as a highly suitable model for primary infections and rechallenges in humans to uncover further mechanisms of immune aging in the elderly.

Acknowledgments

We thank Nadine Litzba, Meaghan Stolk, Regina Stark, and Julian Braun for critical reading of the manuscript and Beate Möwes, Karolina Grzeschik, Manuela Krüger, Anne Ihlenfeld, David Mayer, Cecilia Bozzetti, Dominika Rachwalik, Heike Hirseland, and especially the Berlin-Brandenburg Center for Regenerative Therapies Flow Cytometry Laboratory for expert technical assistance. We further thank all vaccinees for participation in this study.

Disclosures

The authors have no financial conflicts of interest.

References

1. Fulop, T., A. Larbi, R. Kotb, F. de Angelis, and G. Pawelec. 2011. Aging, immunity, and cancer. *Discov. Med.* 11: 537–550.
2. Goronzy, J. J., and C. M. Weyand. 2012. Immune aging and autoimmunity. *Cell. Mol. Life Sci.* 69: 1615–1623.
3. Gavazzi, G., and K. H. Krause. 2002. Ageing and infection. *Lancet Infect. Dis.* 2: 659–666.
4. Maue, A. C., E. J. Yager, S. L. Swain, D. L. Woodland, M. A. Blackman, and L. Haynes. 2009. T-cell immunosenescence: lessons learned from mouse models of aging. *Trends Immunol.* 30: 301–305.

5. Wertheimer, A. M., J. L. Uhrlaub, A. Hirsch, G. Medigeshi, J. Sprague, A. Legasse, J. Wilk, C. A. Wiley, P. Didier, R. B. Tesh, et al. 2010. Immune response to the West Nile virus in aged non-human primates. *PLoS One* 5: e15514.
6. Goronzy, J. J., and C. M. Weyand. 2013. Understanding immunosenescence to improve responses to vaccines. *Nat. Immunol.* 14: 428–436.
7. Vallejo, A. N. 2011. Immunological hurdles of ageing: indispensable research of the human model. *Ageing Res. Rev.* 10: 315–318.
8. Brunner, S., D. Herndler-Brandstetter, B. Weinberger, and B. Grubeck-Loebenstein. 2011. Persistent viral infections and immune aging. *Ageing Res. Rev.* 10: 362–369.
9. Weinberger, B., and B. Grubeck-Loebenstein. 2012. Vaccines for the elderly. *Clin. Microbiol. Infect.* 18(Suppl. 5): 100–108. doi:10.1111/j.1469-0691.2012.03944.x
10. Hainz, U., B. Jenewein, E. Asch, K. P. Pfeiffer, P. Berger, and B. Grubeck-Loebenstein. 2005. Insufficient protection for healthy elderly adults by tetanus and TBE vaccines. *Vaccine* 23: 3232–3235.
11. Blackman, M. A., and D. L. Woodland. 2011. The narrowing of the CD8 T cell repertoire in old age. *Curr. Opin. Immunol.* 23: 537–542.
12. Cicin-Sain, L., S. Smyk-Pearson, N. Currier, L. Byrd, C. Koudelka, T. Robinson, G. Swarbrick, S. Tackitt, A. Legasse, M. Fischer, et al. 2010. Loss of naive T cells and repertoire constriction predict poor response to vaccination in old primates. *J. Immunol.* 184: 6739–6745.
13. Yager, E. J., M. Ahmed, K. Lanzer, T. D. Randall, D. L. Woodland, and M. A. Blackman. 2008. Age-associated decline in T cell repertoire diversity leads to holes in the repertoire and impaired immunity to influenza virus. *J. Exp. Med.* 205: 711–723.
14. Shaw, A. C., D. R. Goldstein, and R. R. Montgomery. 2013. Age-dependent dysregulation of innate immunity. *Nat. Rev. Immunol.* 13: 875–887.
15. Kohler, S., N. Bethke, M. Böthe, S. Sommerick, M. Frentsch, C. Romagnani, M. Niedrig, and A. Thiel. 2012. The early cellular signatures of protective immunity induced by live viral vaccination. *Eur. J. Immunol.* 42: 2363–2373.
16. Ahmed, R., and R. S. Akondy. 2011. Insights into human CD8(+) T-cell memory using the yellow fever and smallpox vaccines. *Immunol. Cell Biol.* 89: 340–345.
17. Liprandi, F., and R. Walder. 1983. Replication of virulent and attenuated strains of yellow fever virus in human monocytes and macrophage-like cells (U937). *Arch. Virol.* 76: 51–61.
18. Gaucher, D., R. Therrien, N. Kettaf, B. R. Angermann, G. Boucher, A. Filali-Mouhim, J. M. Moser, R. S. Mehta, D. R. Drake, III, E. Castro, et al. 2008. Yellow fever vaccine induces integrated multilineage and polyfunctional immune responses. *J. Exp. Med.* 205: 3119–3131.
19. Poland, J. D., C. H. Calisher, T. P. Monath, W. G. Downs, and K. Murphy. 1981. Persistence of neutralizing antibody 30-35 years after immunization with 17D yellow fever vaccine. *Bull. World Health Organ.* 59: 895–900.
20. Monath, T. P. 2012. Review of the risks and benefits of yellow fever vaccination including some new analyses. *Expert Rev. Vaccines* 11: 427–448.
21. Barwick Eidex, R., Yellow Fever Vaccine Safety Working Group. 2004. History of thymoma and yellow fever vaccination. *Lancet* 364: 936.
22. Khromava, A. Y., R. B. Eidex, L. H. Weld, K. S. Kohl, R. D. Bradshaw, R. T. Chen, and M. S. Cetron, Yellow Fever Vaccine Safety Working Group. 2005. Yellow fever vaccine: an updated assessment of advanced age as a risk factor for serious adverse events. *Vaccine* 23: 3256–3263.
23. Domingo, C., P. Patel, J. Yillah, M. Weidmann, J. A. Méndez, E. R. Nakouné, and M. Niedrig. 2012. Advanced yellow fever virus genome detection in point-of-care facilities and reference laboratories. *J. Clin. Microbiol.* 50: 4054–4060.
24. Reinhardt, B., R. Jaspert, M. Niedrig, C. Kostner, and J. L'age-Stehr. 1998. Development of viremia and humoral and cellular parameters of immune activation after vaccination with yellow fever virus strain 17D: a model of human flavivirus infection. *J. Med. Virol.* 56: 159–167.
25. Reed, L. J., and H. Muench. 1938. A simple method of estimating fifty percent endpoints. *Am. J. Hyg.* 27: 493–497.
26. Miller, J. D., R. G. van der Most, R. S. Akondy, J. T. Glidewell, S. Albott, D. Masopust, K. Murali-Krishna, P. L. Mahar, S. Edupuganti, S. Lalor, et al. 2008. Human effector and memory CD8+ T cell responses to smallpox and yellow fever vaccines. *Immunity* 28: 710–722.
27. Akondy, R. S., N. D. Monson, J. D. Miller, S. Edupuganti, D. Teuwen, H. Wu, F. Quyyumi, S. Garg, J. D. Altman, C. Del Rio, et al. 2009. The yellow fever virus vaccine induces a broad and polyfunctional human memory CD8+ T cell response. *J. Immunol.* 183: 7919–7930.
28. Akondy, R. S., P. L. Johnson, H. I. Nakaya, S. Edupuganti, M. J. Mulligan, B. Lawson, J. D. Miller, B. Pulendran, R. Antia, and R. Ahmed. 2015. Initial viral load determines the magnitude of the human CD8 T cell response to yellow fever vaccination. *Proc. Natl. Acad. Sci. USA* 112: 3050–3055.
29. Blom, K., M. Braun, M. A. Ivarsson, V. D. Gonzalez, K. Falconer, M. Moll, H. G. Ljunggren, J. Michaëlsson, and J. K. Sandberg. 2013. Temporal dynamics of the primary human T cell response to yellow fever virus 17D as it matures from an effector- to a memory-type response. *J. Immunol.* 190: 2150–2158.
30. Roederer, M., J. L. Nozzi, and M. C. Nason. 2011. SPICE: exploration and analysis of post-cytometric complex multivariate datasets. *Cytometry A* 79: 167–174.
31. R_Core_Team. 2012. R: A language and environment for statistical computing. R Foundation for Statistical Computing, Vienna, Austria.
32. Zaunders, J. J., W. B. Dyer, M. L. Munier, S. Ip, J. Liu, E. Amyes, W. Rawlinson, R. De Rose, S. J. Kent, J. S. Sullivan, et al. 2006. CD127+CCR5+CD38+++ CD4+ Th1 effector cells are an early component of the primary immune response to vaccinia virus and precede development of interleukin-2+ memory CD4+ T cells. *J. Virol.* 80: 10151–10161.
33. Fagnoni, F. F., R. Vescovini, G. Passeri, G. Bologna, M. Pedrazzoni, G. Lavagetto, A. Casti, C. Franceschi, M. Passeri, and P. Sansoni. 2000. Shortage of circulating naive CD8(+) T cells provides new insights on immunodeficiency in aging. *Blood* 95: 2860–2868.
34. Appay, V., and D. Sauce. 2014. Naive T cells: the crux of cellular immune aging? *Exp. Gerontol.* 54: 90–93.
35. Bassi, M. R., M. Kongsgaard, M. A. Steffensen, C. Fenger, M. Rasmussen, K. Skjødt, B. Finsen, A. Stryhn, S. Buus, J. P. Christensen, and A. R. Thomsen. 2015. CD8+ T cells complement antibodies in protecting against yellow fever virus. *J. Immunol.* 194: 1141–1153.
36. Seder, R. A., P. A. Darrah, and M. Roederer. 2008. T-cell quality in memory and protection: implications for vaccine design. *Nat. Rev. Immunol.* 8: 247–258.
37. Boyd, A., J. R. Almeida, P. A. Darrah, D. Sauce, R. A. Seder, V. Appay, G. Gorochov, and M. Larsen. 2015. Pathogen-Specific T Cell Polyfunctionality Is a Correlate of T Cell Efficacy and Immune Protection. [Published erratum appears in 2015 *PLoS ONE.* 10: e0138395.] *PLoS One* 10: e0128714.
38. Darrah, P. A., D. T. Patel, P. M. De Luca, R. W. Lindsay, D. F. Davey, B. J. Flynn, S. T. Hoff, P. Andersen, S. G. Reed, S. L. Morris, et al. 2007. Multifunctional TH1 cells define a correlate of vaccine-mediated protection against *Leishmania major. Nat. Med.* 13: 843–850.
39. Kannanganat, S., C. Ibegbu, L. Chennareddi, H. L. Robinson, and R. R. Amara. 2007. Multiple-cytokine-producing antiviral CD4 T cells are functionally superior to single-cytokine-producing cells. *J. Virol.* 81: 8468–8476.
40. Kimmig, S., G. K. Przybylski, C. A. Schmidt, K. Laurisch, B. Möwes, A. Radbruch, and A. Thiel. 2002. Two subsets of naive T helper cells with distinct T cell receptor excision circle content in human adult peripheral blood. *J. Exp. Med.* 195: 789–794.
41. Kohler, S., U. Wagner, M. Pierer, S. Kimmig, B. Oppmann, B. Möwes, K. Jülke, C. Romagnani, and A. Thiel. 2005. Post-thymic in vivo proliferation of naive CD4+ T cells constrains the TCR repertoire in healthy human adults. *Eur. J. Immunol.* 35: 1987–1994.
42. Querec, T. D., R. S. Akondy, E. K. Lee, W. Cao, H. I. Nakaya, D. Teuwen, A. Pirani, K. Gernert, J. Deng, B. Marzolf, et al. 2009. Systems biology approach predicts immunogenicity of the yellow fever vaccine in humans. *Nat. Immunol.* 10: 116–125.
43. Muyanja, E., A. Ssemaganda, P. Ngauv, R. Cubas, H. Perrin, D. Srinivasan, G. Canderan, B. Lawson, J. Kopycinski, A. S. Graham, et al. 2014. Immune activation alters cellular and humoral responses to yellow fever 17D vaccine. *J. Clin. Invest.* 124: 3147–3158.
44. Trzonkowski, P., J. Myśliwska, E. Szmit, J. Wieckiewicz, K. Lukaszuk, L. B. Brydak, M. Machała, and A. Myśliwski. 2003. Association between cytomegalovirus infection, enhanced proinflammatory response and low level of anti-hemagglutinins during the anti-influenza vaccination–an impact of immunosenescence. *Vaccine* 21: 3826–3836.
45. Derhovanessian, E., H. Theeten, K. Hähnel, P. Van Damme, N. Cools, and G. Pawelec. 2013. Cytomegalovirus-associated accumulation of late-differentiated CD4 T-cells correlates with poor humoral response to influenza vaccination. *Vaccine* 31: 685–690.
46. Fülöp, T., A. Larbi, and G. Pawelec. 2013. Human T cell aging and the impact of persistent viral infections. *Front. Immunol.* 4: 271.
47. Roukens, A. H., D. Soonawala, S. A. Joosten, A. W. de Visser, X. Jiang, K. Dirksen, M. de Gruijter, J. T. van Dissel, P. J. Bredenbeek, and L. G. Visser. 2011. Elderly subjects have a delayed antibody response and prolonged viraemia following yellow fever vaccination: a prospective controlled cohort study. *PLoS One* 6: e27753.
48. Pulendran, B., J. Miller, T. D. Querec, R. Akondy, N. Moseley, O. Laur, J. Glidewell, N. Monson, T. Zhu, H. Zhu, et al. 2008. Case of yellow fever vaccine–associated viscerotropic disease with prolonged viremia, robust adaptive immune responses, and polymorphisms in CCR5 and RANTES genes. *J. Infect. Dis.* 198: 500–507.
49. Po, J. L., E. M. Gardner, F. Anaraki, P. D. Katsikis, and D. M. Murasko. 2002. Age-associated decrease in virus-specific CD8+ T lymphocytes during primary influenza infection. *Mech. Ageing Dev.* 123: 1167–1181.
50. Monath, T. P., F. Guirakhoo, R. Nichols, S. Yoksan, R. Schrader, C. Murphy, P. Blum, S. Woodward, K. McCarthy, D. Mathis, et al. 2003. Chimeric live, attenuated vaccine against Japanese encephalitis (ChimeriVax-JE): phase 2 clinical trials for safety and immunogenicity, effect of vaccine dose and schedule, and memory response to challenge with inactivated Japanese encephalitis antigen. *J. Infect. Dis.* 188: 1213–1230.
51. Nikolich-Žugich, J., G. Li, J. L. Uhrlaub, K. R. Renkema, and M. J. Smithey. 2012. Age-related changes in CD8 T cell homeostasis and immunity to infection. *Semin. Immunol.* 24: 356–364.
52. Murasko, D. M., and J. Jiang. 2005. Response of aged mice to primary virus infections. *Immunol. Rev.* 205: 285–296.
53. Brien, J. D., J. L. Uhrlaub, A. Hirsch, C. A. Wiley, and J. Nikolich-Zugich. 2009. Key role of T cell defects in age-related vulnerability to West Nile virus. *J. Exp. Med.* 206: 2735–2745.
54. Smithey, M. J., K. R. Renkema, B. D. Rudd, and J. Nikolich-Žugich. 2011. Increased apoptosis, curtailed expansion and incomplete differentiation of CD8+ T cells combine to decrease clearance of *L. monocytogenes* in old mice. *Eur. J. Immunol.* 41: 1352–1364.
55. Parsons, R., A. Lelic, L. Hayes, A. Carter, L. Marshall, C. Evelegh, M. Drebot, M. Andonova, C. McMurtrey, W. Hildebrand, et al. 2008. The memory T cell response to West Nile virus in symptomatic humans following natural infection is not influenced by age and is dominated by a restricted set of CD8+ T cell epitopes. *J. Immunol.* 181: 1563–1572.
56. Piazza, P., C. P. McMurtrey, A. Lelic, R. L. Cook, R. Hess, E. Yablonsky, L. Borowski, M. B. Loeb, J. L. Bramson, W. H. Hildebrand, and C. R. Rinaldo. 2010. Surface phenotype and functionality of WNV specific T cells differ with age and disease severity. *PLoS One* 5: e15343.

57. Lelic, A., C. P. Verschoor, M. Ventresca, R. Parsons, C. Evelegh, D. Bowdish, M. R. Betts, M. B. Loeb, and J. L. Bramson. 2012. The polyfunctionality of human memory CD8+ T cells elicited by acute and chronic virus infections is not influenced by age. *PLoS Pathog.* 8: e1003076.
58. Lanzer, K. G., L. L. Johnson, D. L. Woodland, and M. A. Blackman. 2014. Impact of ageing on the response and repertoire of influenza virus-specific CD4 T cells. *Immun. Ageing* 11: 9.
59. Pérez-Cabezas, B., M. Naranjo-Gómez, M. A. Fernández, J. R. Grífols, R. Pujol-Borrell, and F. E. Borràs. 2007. Reduced numbers of plasmacytoid dendritic cells in aged blood donors. *Exp. Gerontol.* 42: 1033–1038.
60. Garbe, K., K. Bratke, S. Wagner, J. C. Virchow, and M. Lommatzsch. 2012. Plasmacytoid dendritic cells and their Toll-like receptor 9 expression selectively decrease with age. *Hum. Immunol.* 73: 493–497.
61. Seidler, S., H. W. Zimmermann, M. Bartneck, C. Trautwein, and F. Tacke. 2010. Age-dependent alterations of monocyte subsets and monocyte-related chemokine pathways in healthy adults. *BMC Immunol.* 11: 30.
62. Monath, T. P., M. S. Cetron, K. McCarthy, R. Nichols, W. T. Archambault, L. Weld, and P. Bedford. 2005. Yellow fever 17D vaccine safety and immunogenicity in the elderly. *Hum. Vaccin.* 1: 207–214.
63. Monath, T. P., R. Nichols, W. T. Archambault, L. Moore, R. Marchesani, J. Tian, R. E. Shope, N. Thomas, R. Schrader, D. Furby, and P. Bedford. 2002. Comparative safety and immunogenicity of two yellow fever 17D vaccines (ARILVAX and YF-VAX) in a phase III multicenter, double-blind clinical trial. *Am. J. Trop. Med. Hyg.* 66: 533–541.
64. Hacker, U. T., T. Jelinek, S. Erhardt, A. Eigler, G. Hartmann, H. D. Nothdurft, and S. Endres. 1998. In vivo synthesis of tumor necrosis factor-alpha in healthy humans after live yellow fever vaccination. *J. Infect. Dis.* 177: 774–778.
65. Bruni, D., M. Chazal, L. Sinigaglia, L. Chauveau, O. Schwartz, P. Desprès, and N. Jouvenet. 2015. Viral entry route determines how human plasmacytoid dendritic cells produce type I interferons. *Sci. Signal.* 8: ra25.
66. Solana, R., R. Tarazona, I. Gayoso, O. Lesur, G. Dupuis, and T. Fulop. 2012. Innate immunosenescence: effect of aging on cells and receptors of the innate immune system in humans. *Semin. Immunol.* 24: 331–341.
67. Agrawal, A., and S. Gupta. 2011. Impact of aging on dendritic cell functions in humans. *Ageing Res. Rev.* 10: 336–345.
68. Qian, F., X. Wang, L. Zhang, A. Lin, H. Zhao, E. Fikrig, and R. R. Montgomery. 2011. Impaired interferon signaling in dendritic cells from older donors infected in vitro with West Nile virus. *J. Infect. Dis.* 203: 1415–1424.
69. Smithey, M. J., G. Li, V. Venturi, M. P. Davenport, and J. Nikolich-Žugich. 2012. Lifelong persistent viral infection alters the naive T cell pool, impairing CD8 T cell immunity in late life. *J. Immunol.* 189: 5356–5366.
70. Cicin-Sain, L., J. D. Brien, J. L. Uhrlaub, A. Drabig, T. F. Marandu, and J. Nikolich-Zugich. 2012. Cytomegalovirus infection impairs immune responses and accentuates T-cell pool changes observed in mice with aging. *PLoS Pathog.* 8: e1002849.
71. Who. 2015. Vaccines and vaccination against yellow fever: WHO Position Paper, June 2013–recommendations. *Vaccine* 33: 76–77.
72. Jean, C. M., S. Honarmand, J. K. Louie, and C. A. Glaser. 2007. Risk factors for West Nile virus neuroinvasive disease, California, 2005. *Emerg. Infect. Dis.* 13: 1918–1920.
73. Peiris, J. S., C. M. Chu, V. C. Cheng, K. S. Chan, I. F. Hung, L. L. Poon, K. I. Law, B. S. Tang, T. Y. Hon, C. S. Chan, et al; HKU/UCH SARS Study Group. 2003. Clinical progression and viral load in a community outbreak of coronavirus-associated SARS pneumonia: a prospective study. *Lancet* 361: 1767–1772.
74. Liniger, M., A. Zuniga, and H. Y. Naim. 2007. Use of viral vectors for the development of vaccines. *Expert Rev. Vaccines* 6: 255–266.